# Function and Molecular Mechanism of Acetylation in Autophagy Regulation

Cong Yi,[1] Meisheng Ma,[1] Leili Ran,[1] Jingxiang Zheng,[1] Jingjing Tong,[1] Jing Zhu,[1] Chengying Ma,[2] Yufen Sun,[1] Shaojin Zhang,[1] Wenzhi Feng,[1] Liyuan Zhu,[1] Yan Le,[1] Xingqi Gong,[2] Xianghua Yan,[3] Bing Hong,[4] Fen-Jun Jiang,[4] Zhiping Xie,[4] Di Miao,[5] Haiteng Deng,[5] Li Yu[1]*

Protein acetylation emerged as a key regulatory mechanism for many cellular processes. We used genetic analysis of *Saccharomyces cerevisiae* to identify Esa1 as a histone acetyltransferase required for autophagy. We further identified the autophagy signaling component Atg3 as a substrate for Esa1. Specifically, acetylation of K19 and K48 of Atg3 regulated autophagy by controlling Atg3 and Atg8 interaction and lipidation of Atg8. Starvation induced transient K19-K48 acetylation through spatial and temporal regulation of the localization of acetylase Esa1 and the deacetylase Rpd3 on pre-autophagosomal structures (PASs) and their interaction with Atg3. Attenuation of K19-K48 acetylation was associated with attenuation of autophagy. Increased K19-K48 acetylation after deletion of the deacetylase Rpd3 caused increased autophagy. Thus, protein acetylation contributes to control of autophagy.

Autophagy is a degradation pathway conserved from yeast to mammals (*1*). Eighteen essential autophagy genes have been identified in yeast (*2*). Acetylation is reported to regulate autophagy (*3*, *4*). Treating cells with deacetylase inhibitors can induce autophagy (*5*), whereas P300-mediated acetylation of autophagy proteins appears to have an inhibitory role in autophagy (*3*). Thus, the role of acetylation in autophagy remains unclear.

We investigated whether any of the eight histone acetyltransferase (HAT) complexes in *Saccharomyces cerevisae* are required for autophagy. By analyzing deletion or mutants of catalytic subunits of all eight HATs, we identified Esa1, the catalytic subunit of NuA4, as a HAT that is required for autophagy (Fig. 1A). Nitrogen starvation–induced green fluorescent protein (GFP)–Atg8 vacuoles translocation and cleavage were impaired in *esa1-1*, a temperature-sensitive mutant strain of Esa1 (Fig. 1, B to D), which indicated that Esa1 regulates autophagy. Epl1, a regulatory subunit of NuA4, is also required for autophagy (Fig. 1, E to G). Autophagy induced by other cues was also impaired in *esa1-1* or *epl1-1* (figs. S1 and S2), and depletion of Tip60, the mammalian homolog of Esa1, impaired starvation-induced autophagy in normal rat kidney (NRK) cells (fig. S3). Thus, Esa1-mediated acetylation is required in an evolutionarily conserved manner for autophagy.

We tested whether Esa1 regulates autophagy by directly acetylating autophagy proteins. The 18 essential autophagy genes can be classified into several groups according to their function (*2*). By testing which function is impaired in *esa1-1*, we could narrow our search for the Esa1 substrate (fig. S4A). Rapamycin-induced autophagy was impaired in *esa1-1* (fig. S4, B and C), indicating

[1]State Key Laboratory of Biomembrane and Membrane Biotechnology, Tsinghua University–Peking University Joint Center for Life Sciences, School of Life Sciences, Tsinghua University, Beijing 100084, China. [2]Center of Structural Biology, Tsinghua University, Beijing 100084, China. [3]College of Animal Sciences and Technology, Huazhong Agricultural University, Wuhan, Hubei 430070, China. [4]School of Medicine, Nankai University, 94 Wei-Jin Road, Tianjin 300071, China. [5]Proteomics Facility, School of Life Sciences, Tsinghua University, Beijing 100084, China.

*To whom correspondence should be addressed. E-mail: liyulab@mail.tsinghua.edu.cn

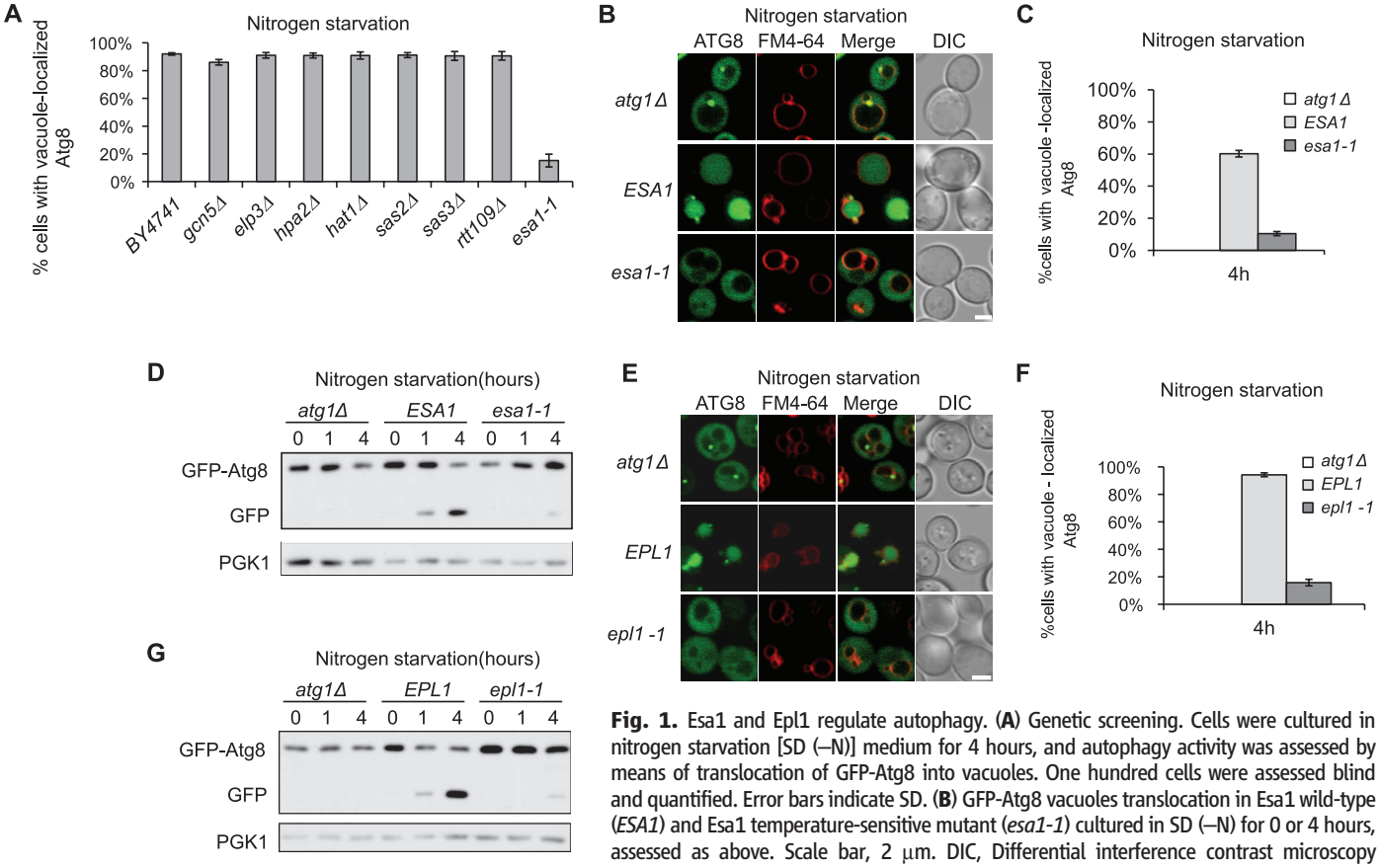


**Fig. 1.** Esa1 and Epl1 regulate autophagy. (**A**) Genetic screening. Cells were cultured in nitrogen starvation [SD (–N)] medium for 4 hours, and autophagy activity was assessed by means of translocation of GFP-Atg8 into vacuoles. One hundred cells were assessed blind and quantified. Error bars indicate SD. (**B**) GFP-Atg8 vacuoles translocation in Esa1 wild-type (*ESA1*) and Esa1 temperature-sensitive mutant (*esa1-1*) cultured in SD (–N) for 0 or 4 hours, assessed as above. Scale bar, 2 μm. DIC, Differential interference contrast microscopy images. (**C**) One hundred cells from (B) were quantified for autophagy as above. (**D**) Cells from (B) were analyzed by means of Western blot for GFP-Atg8 cleavage. (**E**) GFP-Atg8 vacuoles translocation in *EPL1* and *epl1-1* cells was assessed as above. Scale bar, 2 μm. (**F**) One hundred cells from (E) were quantified for autophagy as above. (**G**) Cells from (E) were analyzed by means of Western blot for GFP-Atg8 cleavage.

that acetylation regulates molecular events downstream of the mammalian target of rapamycin (mTOR) complex. Atg1 protein puncta formation was normal in *esa1-1* (fig. S4, D and E); formation of Atg8 puncta was reduced in *esa1-1* but not in cells expressing a catalytically inactive form of the kinase Atg1 (fig. S4F), suggesting that acetylation probably regulates steps downstream of the Atg1 complex. Normal phosphatidylinositol 3-phosphate (PI3P) production and Atg6 localization in *esa1-1* indicated that the function of the PI3K complex was unchanged in *esa1-1* (fig. S4, G and H). Thus, the two ubiquitin-like pathways probably contain the substrate of Esa1.

We directly tested the acetylation status of proteins from the two ubiquitin-like pathways; Atg3, Atg5, and Atg8 are acetylated when grown in nutrient-rich medium (Fig. 2A). After starvation, acetylation of Atg3 increased, although the acetylation of other proteins was reduced or unchanged (Fig. 2A). Acetylation level of Atg3 is reduced in *esa1-1* (Fig. 2B), indicating that Atg3 may be a substrate of Esa1. To determine the acetylation site of Atg3, we purified a fusion protein in which Atg3 was fused to glutathione S-transferase (GST-Atg3) from starved yeast (fig. S5); mass spectrometry showed that K19, K48, and K183 were acetylated (Fig. 2C). (Single-letter abbreviations for the amino acid residues are as follows: A, Ala; C, Cys; D, Asp; E, Glu; F, Phe; G, Gly; H, His; I, Ile; K, Lys; L, Leu; M, Met; N, Asn; P, Pro; Q, Gln; R, Arg; S, Ser; T, Thr; V, Val; W, Trp; and Y, Tyr. In the mutants, other amino acids were substituted at certain locations; for example, K19R indicates that lysine at position 19 was replaced by arginine.) We also analyzed mutants expressing Atg3 proteins in which acetylated lysines were replaced by arginines. Acetylation of $Atg3^{K19R\text{-}K48R}$ and $Atg3^{K19R\text{-}K48R\text{-}K183R}$ mutants was reduced (Fig. 3A). In vitro Esa1 acetylates Atg3 and acetylation of $Atg3^{K19R\text{-}K48R}$ and $Atg3^{K19R\text{-}K48R\text{-}K183R}$ was reduced (Fig. 3B).

To test which acetylation site is critical for autophagy, we expressed plasmids encoding *ATG3* [wild-type (WT)], $atg3^{K19R}$, $atg3^{K48R}$, $atg3^{K183R}$, $atg3^{K19R\text{-}K48R}$, and $atg3^{K19R\text{-}K48R\text{-}K183R}$ in cells in which the Atg3 gene was deleted. Autophagy in *atg3*Δ cells was fully rescued by expression of wild-type Atg3. However, cells expression of $atg3^{K19R\text{-}K48R}$ or $atg3^{K19R\text{-}K48R\text{-}K183R}$ had impaired autophagy induced by various cues (Fig. 3, C to E, and fig. S6), suggesting that K19-K48 acetylation of Atg3 is critical for autophagy.

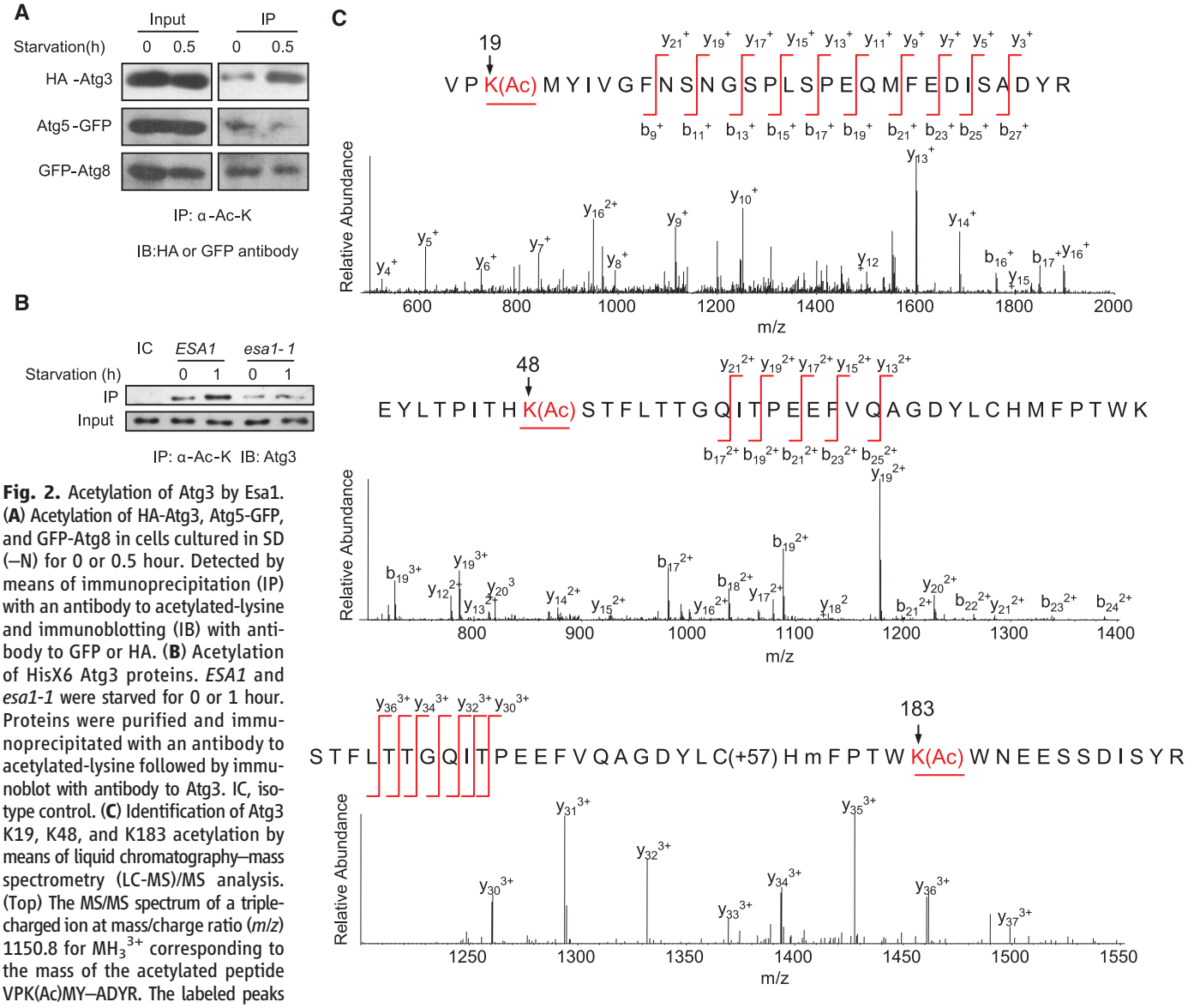


**Fig. 2.** Acetylation of Atg3 by Esa1. (**A**) Acetylation of HA-Atg3, Atg5-GFP, and GFP-Atg8 in cells cultured in SD (–N) for 0 or 0.5 hour. Detected by means of immunoprecipitation (IP) with an antibody to acetylated-lysine and immunoblotting (IB) with antibody to GFP or HA. (**B**) Acetylation of HisX6 Atg3 proteins. *ESA1* and *esa1-1* were starved for 0 or 1 hour. Proteins were purified and immunoprecipitated with an antibody to acetylated-lysine followed by immunoblot with antibody to Atg3. IC, isotype control. (**C**) Identification of Atg3 K19, K48, and K183 acetylation by means of liquid chromatography–mass spectrometry (LC-MS)/MS analysis. (Top) The MS/MS spectrum of a triple-charged ion at mass/charge ratio (*m/z*) 1150.8 for $MH_3^{3+}$ corresponding to the mass of the acetylated peptide VPK(Ac)MY–ADYR. The labeled peaks correspond to masses of *y* ions of acetylated peptide fragments. (Middle) The MS/MS spectrum of a quintuple-charged ion at *m/z* 907.1 for $MH_5^{5+}$ corresponding to the mass of the acetylated peptide EYLTPITHK(Ac)–TWK. (Bottom) The MS/MS spectrum of a quadruple-charged ion at *m/z* 1208.05 for $MH_4^{4+}$ corresponding to the mass of the acetylated peptide STFL–WK(Ac) WNEESSDISYR.

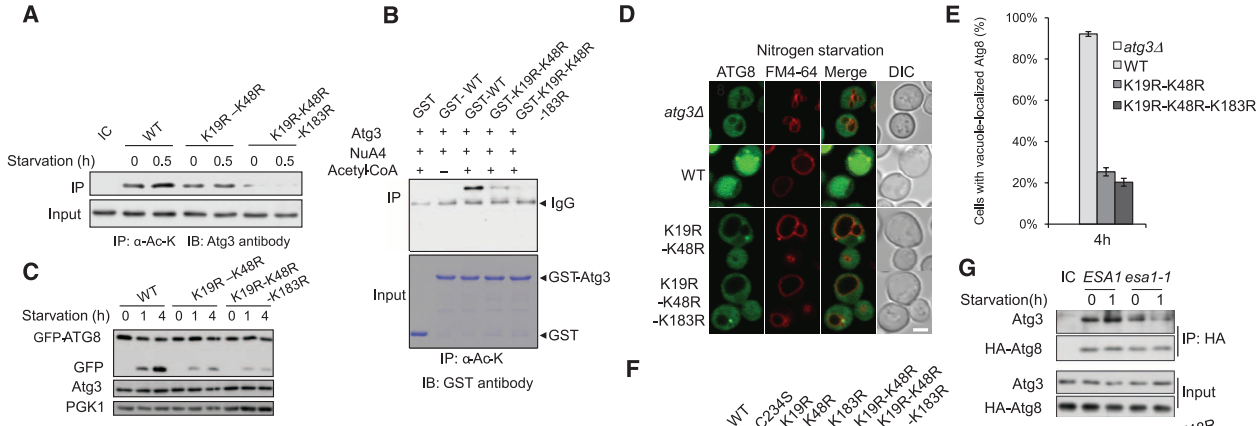


**Fig. 3.** Effect of Atg3 acetylation on Atg3-Atg8 interaction. (**A**) Acetylation of Atg3 mutants. *atg3*Δ+*ATG3* WT (WT), *atg3*Δ+*atg3*$^{K19R\text{-}K48R}$ (K19R-K48R), and *atg3*Δ+*atg3*$^{K19R\text{-}K48R\text{-}K183R}$ (K19R-K48R-K183R) were starved for 0.5 hour. Proteins from lysates were immunoprecipitated with antibody to acetylated-lysine followed by immunoblotting with antibody to Atg3. (**B**) In vitro acetylation of purified GST, GST-Atg3 WT, GST-Atg3$^{K19R\text{-}K48R}$, and GST-Atg3$^{K19R\text{-}K48R\text{-}K183R}$ proteins was measured by means of immunoprecipitation with antibody to acetylated-lysine followed by immunoblotting with GST antibody. (**C** and **D**) Autophagy in *atg3*Δ, *atg3*Δ+*ATG3* WT, *atg3*Δ+*atg3*$^{K19R\text{-}K48R}$, and *atg3*Δ+*atg3*$^{K19R\text{-}K48R\text{-}K183R}$ cells cultured in SD (–N) for various times were analyzed by means of Western blot for (C) GFP-Atg8 cleavage and (D) translocation of GFP-Atg8 into vacuoles. Scale bar, 2 μm. (**E**) One hundred cells from (D) were quantified for autophagy. (**F**) Lipidation of Atg8. Purified Atg3 and Atg3 mutants, Atg7, Atg8, and liposomes were incubated for in vitro Atg8 lipidation and analyzed by SDS–polyacrylamide gel electrophoresis. (**G** and **H**) Association of Atg3 and Atg8 in (G) *ESA1* and *esa1-1* or (H) *atg3*Δ+*ATG3* WT and *atg3*Δ+*atg3*$^{K19R\text{-}K48R}$ cells expressing HA-Atg8. Cells were cultured in SD (–N) for 0 or 1 hour. Cell lysates were immunoprecipitated with antibody to HA and analyzed by means of Western blot by using an antibody to Atg3.

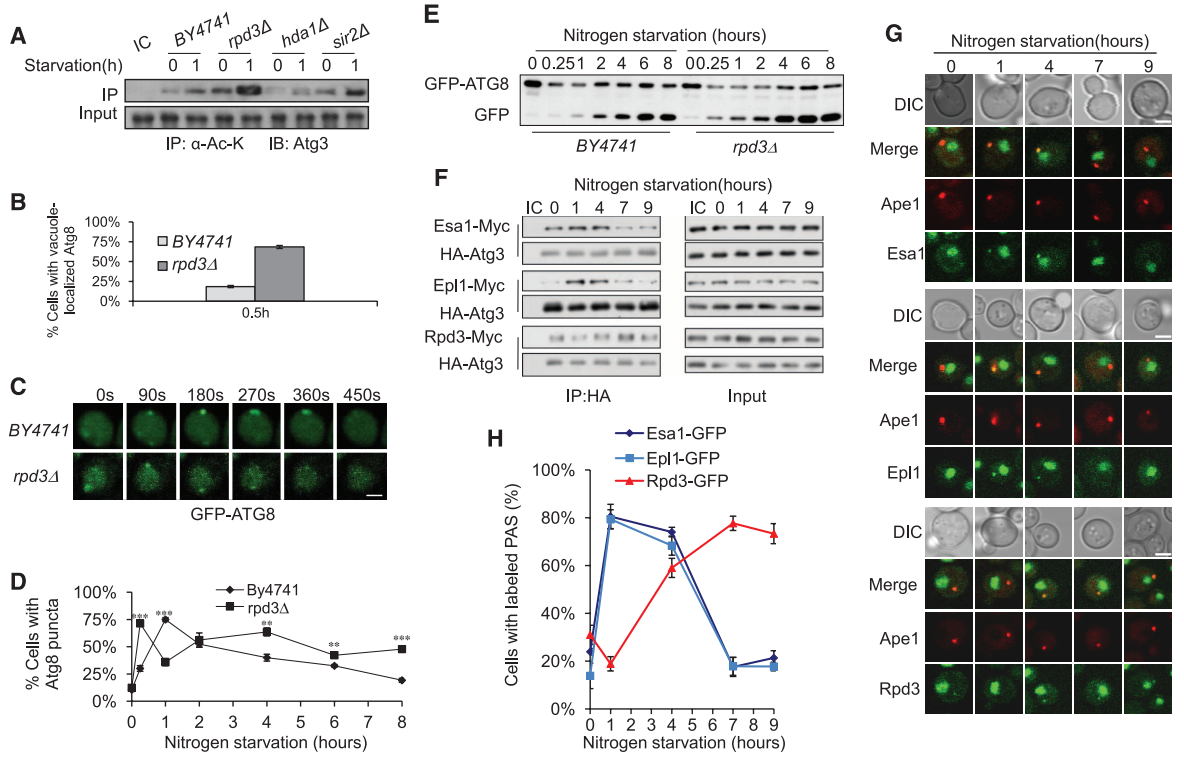


**Fig. 4.** Effect of acetylation on duration of starvation-induced autophagy, and dynamic Atg3 interaction and PAS localization of Esa1, Epl1, and Rpd3. (**A**) Acetylation of GST-Atg3 in wild type, *rpd3*Δ, *hda1*Δ, and *sir2*Δ expressing GST-Atg3. Cells were starved for 0 or 1 hour. Total GST-Atg3 was purified and immunoprecipitated with an antibody to acetylated-lysine followed by immunoblotting with antibody to Atg3. (**B**) Translocation of GFP-Atg8 into vacuoles in 100 wild-type or *rpd3*Δ cells cultured in SD (–N) for 0.5 hour was assessed and quantified. (**C**) Duration of Atg8 puncta in wild-type and *rpd3*Δ cells cultured in SD (–N) for 1 hour. Scale bar, 2 μm. (**D**) Time course of Atg8 puncta formation in wild-type *rpd3*Δ cells cultured in SD (–N) medium. $^{**}P < 0.01$, $^{***}P < 0.001$ (Student's *t* test). (**E**) Wild-type and *rpd3*Δ cells cultured in SD (ΔN) for various time and were assessed for GFP-Atg8 cleavage. (**F**) Interactions of (top) Esa1-Myc and HA-Atg3, (middle) Epl1-Myc and HA-Atg3, and (bottom) Rpd3-Myc and HA-Atg3. Cell lysates were immunoprecipitated with antibody against HA and analyzed by means of Western blot by using an antibody against Myc. (**G**) Time course of localization of (top) Esa1-GFP and Ape1-RFP, (middle) Epl1-GFP and Ape1-RFP, and (bottom) Rpd1-GFP and Ape1-RFP. Scale bar, 2 μm. (**H**) Cells from (G) were quantified for Esa1-GFP–, Epl1-GFP–, and Rpd3-GFP–positive PAS. One hundred Ape1-RFP positive cells were counted. Error bars indicate SD.

Atg3, as the E2-like protein, together with E1-like Atg7 and E3-like Atg5-Atg12 complex covalently conjugate phosphatidylethanolamine (PE) to Atg8 (*6*). Atg8 lipidation reaction can be reconstituted in vitro with recombinant Atg7 and Atg3 (*7*). To exclude the possibility that K-R mutation may affect autophagy by directly disturbing Atg3 enzymatic activity rather than reducing Atg3 acetylation, we assayed the enzymatic activity of recombinant variants of Atg3 in an in vitro Atg8 lipidation reaction. $atg3^{K19R}$, $atg3^{K48R}$, and $atg3^{K19R\text{-}K48R}$ catalyzed Atg8 lipidation, whereas $atg3^{K183R}$ and $atg3^{K19R\text{-}K48R\text{-}K183R}$ mediate little Atg8 lipidation (Fig. 3F). Thus, K183R mutation disrupts the enzymatic activity of Atg3, but K19R and K48R do not. Because both $atg3^{K19R\text{-}K48R}$ and $atg3^{K19R\text{-}K48R\text{-}K183R}$ block autophagy, we conclude that acetylation on K19 and K48 are important for regulation of autophagy, whereas K183 is important for Atg3 enzymatic activity.

Atg8 conjugation to PE requires the interaction of Atg3 with Atg8 (*8*). In *esa1-1*, the interaction between endogenous Atg3 and exogenous tagged Atg8 was reduced, suggesting that acetylation promotes Atg3-Atg8 interaction (Fig. 3G). The interaction between Atg8 and $Atg3^{K19R\text{-}K48R}$ was also reduced (Fig. 3H). Thus, Esa1-mediated Atg3 acetylation appears to influence autophagy through controlling Atg3-Atg8 interaction. However, acetylation of other proteins by Esa1 may also affect autophagy.

Histone deacetylases (HDACs) participate in regulation of protein acetylation. Genetic analysis identified Rpd3 as a negative regulator of autophagy (fig. S7). Acetylation of Atg3 was increased in *rpd3*Δ cells (Fig. 4A), and autophagy was accelerated (Fig. 4B and fig. S8). Time-lapse imaging revealed that the duration of Atg8 puncta was reduced in *rpd3*Δ cells (Fig. 4C and fig. S9). Kinetic studies revealed that Atg3 acetylation was transiently induced by starvation (fig. S10). In contrast, Atg3 acetylation was more sustained in *rpd3*Δ cells (fig. S10), suggesting that attenuation of Atg3 acetylation is mediated by Rpd3. Starvation-induced autophagy was transient in wild-type cells (Fig. 4D). However, Atg8 puncta formed rapidly but more slowly attenuated in *rpd3*Δ cells (Fig. 4D), indicating that deacetylation of Atg3 by Rpd3 may contribute to the attenuation of formation of autophagosome during starvation. As a consequence of constitutive autophagosome formation, Atg8-GFP cleavage is increased in *rpd3*Δ cells (Fig. 4E and fig. S11). Thus, metabolic cues appear to regulate the duration and magnitude of autophagy through temporal control of Atg3 acetylation.

Abundance of Esa1, Epl1, and Rpd3 and the enzymatic activity of Esa1 were not changed during autophagy (fig. S12). We constructed yeast strains in which hemagglutinin (HA)–Atg3 was expressed with Esa1-Myc, Epl1-Myc, and Rpd3-Myc, respectively, in physiological amount. We found weak interaction between Atg3 with Esa1 and Epl1 in yeast before starvation. Starvation transiently increased the interaction between Atg3 and Esa1 or Epl1, which peaked 1 hour after starvation and subsided thereafter (Fig. 4F). We also detected interaction between Atg3 and Rpd3 under nutrient-rich conditions, and starvation enhanced this interaction (Fig. 4F). We proposed that the transient acetylation of Atg3 may result from the dynamic interaction between Atg3 and acetylases. In yeast, most of Atg proteins are located on pre-autophagososmal structures (PASs) under growth or starvation conditions (*9*). PASs are thought to be the site for autophagosome formation and can be labeled with vacuolar hydrolases aminopeptidase I (Ape1) (*10*). Most Esa1, Epl1, and Rpd3 was located on the nucleus with or without nitrogen starvation (*11*, *12*); however, we found that in starved cells a small fraction of Esa1, Epl1, and Rpd3 was located in the cytosol in the form of puncta (Fig. 4G and fig. S13). These punctas appeared to colocalize with Ape1, indicating these punctas were PASs (Fig. 4G and fig. S13). Starvation-induced transient recruitment of Esa1-GFP and Epl1-GFP to the PAS peaked 1 hour after starvation and subsided to prestarvation amount after 7 hours of starvation (Fig. 4G and fig. S13). In contrast, Rpd3-GFP was recruited to PAS on a delayed manner (Fig. 4G and fig. S13).

Acetylation is emerging as an important metabolic regulatory mechanism (*13*, *14*) and is itself tightly regulated in response to metabolism changing (*15*). The TOR pathway provides one signaling pathway to couple autophagy with metabolism status. Acetylation may provide another mechanism (fig. S14).


**References and Notes**

1. D. J. Klionsky, *Nat. Rev. Mol. Cell Biol.* **8**, 931 (2007).
2. Y. Ohsumi, *Tanpakushitsu Kakusan Koso* **51** (suppl.), 1453 (2006).
3. I. H. Lee, T. Finkel, *J. Biol. Chem.* **284**, 6322 (2009).
4. Y. Zhao *et al.*, *Nat. Cell Biol.* **12**, 665 (2010).
5. T. Robert *et al.*, *Nature* **471**, 74 (2011).
6. N. Mizushima *et al.*, *Nature* **395**, 395 (1998).
7. Y. Ichimura *et al.*, *J. Biol. Chem.* **279**, 40584 (2004).
8. M. Yamaguchi *et al.*, *J. Biol. Chem.* **285**, 29599 (2010).
9. K. Suzuki, Y. Ohsumi, *FEBS Lett.* **584**, 1280 (2010).
10. T. Shintani, W. P. Huang, P. E. Stromhaug, D. J. Klionsky, *Dev. Cell* **3**, 825 (2002).
11. L. Galarneau *et al.*, *Mol. Cell* **5**, 927 (2000).
12. S. E. Rundlett *et al.*, *Proc. Natl. Acad. Sci. U.S.A.* **93**, 14503 (1996).
13. Q. Wang *et al.*, *Science* **327**, 1004 (2010).
14. S. Zhao *et al.*, *Science* **327**, 1000 (2010).
15. L. Lv *et al.*, *Mol. Cell* **42**, 719 (2011).



**Acknowledgments:** We are grateful to Y. Ohsumi and H. Nakatogawa for antibodies and plasmids, N. Gao for assistance with protein purification, B. Zhou for providing the yeast deletion library, J. Côté for EPL1 and *epl1-1*, L. Pillus for ESA1 and *esa1-1*, and G. Yang for image processing. This research was supported by 973 Program 2011CB910101 and 2010CB833704; National Science Foundation grants 31030043, 31125018, and 30971484; and Tsinghua University grants 2010THZ0 and 2009THZ03071 to L.Y.; National Science Foundation grant 30971441 to Z.X.; and National Science Foundation grants 31172290 and 31072036 to X.Y.


**Supplementary Materials**

www.sciencemag.org/cgi/content/full/336/6080/474/DC1
Materials and Methods
Figs. S1 to S14
References


22 November 2011; accepted 5 March 2012
10.1126/science.1216990


# GSK3-TIP60-ULK1 Signaling Pathway Links Growth Factor Deprivation to Autophagy


**Shu-Yong Lin,[1]* Terytty Yang Li,[1]* Qing Liu,[1] Cixiong Zhang,[1] Xiaotong Li,[1] Yan Chen,[1] Shi-Meng Zhang,[2] Guili Lian,[1] Qi Liu,[1] Ka Ruan,[1] Zhen Wang,[1] Chen-Song Zhang,[1] Kun-Yi Chien,[3] Jiawei Wu,[4] Qinxi Li,[1] Jiahuai Han,[1] Sheng-Cai Lin[1]†**



**In metazoans, cells depend on extracellular growth factors for energy homeostasis. We found that glycogen synthase kinase-3 (GSK3), when deinhibited by default in cells deprived of growth factors, activates acetyltransferase TIP60 through phosphorylating TIP60-$Ser^{86}$, which directly acetylates and stimulates the protein kinase ULK1, which is required for autophagy. Cells engineered to express $TIP60^{S86A}$ that cannot be phosphorylated by GSK3 could not undergo serum deprivation–induced autophagy. An acetylation-defective mutant of ULK1 failed to rescue autophagy in $ULK1^{-/-}$ mouse embryonic fibroblasts. Cells used signaling from GSK3 to TIP60 and ULK1 to regulate autophagy when deprived of serum but not glucose. These findings uncover an activating pathway that integrates protein phosphorylation and acetylation to connect growth factor deprivation to autophagy.**


Autophagy is an evolutionarily conserved cellular process by which a cell degrades its own organelles and large protein aggregates. Autophagy functions to maintain energy homeostasis under nutrient-poor conditions to allow cell survival (*1*–*4*). Unlike unicellular organisms, metazoans depend on extracellular growth factors to regulate uptake and digestion of environmental nutrients. Withdrawal of growth factors or culture of cells in serum-free medium initiates autophagy (*2*, *5*). Dysregulation of autophagy is also associated with diverse diseases, including cancers and neurodegeneration (*6*). Products of a series of autophagy genes (ATGs) mediate and regulate various aspects of autophagy (*7*–*10*). *ATG1* (*ULK1* and *ULK2* in mammals)